J|A|C|S
ARTICLES

Published on Web 03/14/2008

On the Mechanism of Asymmetric Allylation of Aldehydes with Allyltrichlorosilanes Catalyzed by QUINOX, a Chiral Isoquinoline *N*-Oxide

Andrei V. Malkov,*[,†] Pedro Ramírez-López,[†,‡] Lada Biedermannová (née Bendová),[†,§] Lubomír Rulíšek,*[,||] Lenka Dufková,[†,⊥] Martin Kotora,[#] Fujiang Zhu,[†] and Pavel Kočovský*[,†]

Department of Chemistry, WestChem, Joseph Black Building, University of Glasgow, Glasgow G12 8QQ, Scotland, U.K., Institute of Organic Chemistry and Biochemistry and Gilead Sciences Research Center & IOCB, Academy of Sciences of the Czech Republic, Flemingovo náměstí 2, 16610 Prague 6, Czech Republic, and Department of Organic Chemistry, Charles University, Hlavova 2030, 12840, Prague 2, Czech Republic

Received January 2, 2008; E-mail: amalkov@chem.gla.ac.uk; lubos@uochb.cas.cz; pavelk@chem.gla.ac.uk

Abstract: Allylation of aromatic aldehydes **1a**−**m** with allyl- and crotyl-trichlorosilanes **2**–**4**, catalyzed by the chiral *N*-oxide QUINOX (**9**), has been found to exhibit a significant dependence on the electronics of the aldehyde, with *p*-(trifluoromethyl)benzaldehyde **1g** and its *p*-methoxy counterpart **1h** affording the corresponding homoallylic alcohols **6g**,**h** in 96 and 16% ee, respectively, at −40 °C. The kinetic and computational data indicate that the reaction is likely to proceed via an associative pathway involving neutral, octahedral silicon complex **22** with only one molecule of the catalyst involved in the rate- and selectivity-determining step. The crotylation with (*E*) and (*Z*)-crotyltrichlorosilanes **3** and **4** is highly diastereoselective, suggesting the chairlike transition state **5**, which is supported by computational data. High-level quantum chemical calculations further suggest that attractive aromatic interactions between the catalyst **9** and the aldehyde **1** contribute to the enantiodifferentiation and that the dramatic drop in enantioselectivity, observed with the electron-rich aldehyde **1h**, originates from narrowing the energy gap between the (*R*)- and (*S*)-reaction channels in the associative mechanism (**22**). Overall, a good agreement between the theoretically predicted enantioselectivities for **1a** and **1h** and the experimental data allowed to understand the specific aspects of the reaction mechanism.

Introduction

Allyltrialkylsilanes[1] and stannanes[1,2] react readily at low temperature with aldehydes upon activation of the carbonyl group by a Lewis acid.[1−3] By contrast, allyltrichlorosilane (**2**) and related reagents require activation with a Lewis base that coordinates to the silicon (Scheme 1).[1,4−7] Provided the Lewis base dissociates from the silicon at a sufficient rate, it can act as a catalyst (rather than a stoichiometric reagent). Typical Lewis bases that promote the allylation reaction are the common dipolar aprotic solvents, such as DMF,[4,8] DMSO,[4,5] and HMPA,[5,9] and other substances possessing a strongly Lewis basic oxygen, such as formamides,[4,10,11] urea derivatives,[12] catecholates,[6a] and their chiral modifications;[1] the allylation with allyltrifluorosilane can also be promoted by fluoride.[6a,c,e] Analogous allyl boranes and boronates are more reactive than

[†] University of Glasgow.
[‡] Current address: Departamento de Productos Naturales, IQOG (CSIC), Madrid, Spain.
[§] Exchange student from the Institute of Organic Chemistry and Biochemistry, AVČR.
[||] Institute of Organic Chemistry and Biochemistry, AVČR.
[⊥] Exchange student from Charles University.
[#] Charles University.

(1) (a) For leading reviews, see: Denmark, S. E.; Stavenger, R. A. *Acc. Chem. Res.* **2000**, *33*, 432. (b) Denmark, S. E.; Fu, J. *Chem. Commun.* **2003**, 167. (c) Denmark, S. E.; Fu, J. *Chem. Rev.* **2003**, *103*, 2763. (d) Kennedy, J. W. J.; Hall, D. G. *Angew. Chem., Int. Ed.* **2003**, *42*, 4732.
(2) (a) Marshall, J. A. *Chem. Rev.* **1996**, *96*, 31. (b) Marshall, J. A. In *Organometallics in Synthesis;* Schlosser, M., Ed.; J. Wiley and Sons: Chichester, U.K., 2002; p 399.
(3) (a) For the coordination of the C=O group to Lewis acids (η^1 vs η^2 fashion), see, for example: Shambayati, S.; Crowe, W. E.; Schreiber, S. L. *Angew. Chem., Int. Ed. Engl.* **1990**, *29*, 256. (b) Lenges, C. P.; Brookhart, M.; White, P. S. *Angew. Chem., Int. Ed.* **1999**, *38*, 552.
(4) (a) Kobayashi, S.; Nishio, K. *Tetrahedron Lett.* **1993**, *34*, 3453. (b) Kobayashi, S.; Nishio, K. *J. Org. Chem.* **1994**, *59*, 6620. (c) Kobayashi, S.; Nishio, K. *Synthesis* **1994**, 457.
(5) Denmark, S. E.; Coe, D. M.; Pratt, N. E.; and Griedel, B. D. *J. Org. Chem.* **1994**, *59*, 6161.
(6) (a) Kira, M.; Sato, K.; Sakurai, H. *J. Am. Chem. Soc.* **1988**, *110*, 4599. (b) Kira, M.; Kobayashi, M.; Sakurai, H. *Tetrahedron Lett.* **1987**, *28*, 4081. (c) Sakurai, H. *Synlett* **1989**, 1. (d) Kira, M.; Sato, K.; Sakurai, H. *J. Am. Chem. Soc.* **1990**, *112*, 257. (e) Kira, M.; Zhang, L. C.; Kabuto, C.; Sakurai, H. *Organometallics* **1998**, *17*, 887.
(7) (a) Malkov, A. V.; Kočovský, P. *Eur. J. Org. Chem.* **2007**, 29. (b) Kočovský, P.; Malkov, A. V. In *Enantioselective Organocatalysis*; Dalko, P. I., Ed.; Wiley-VCH: Weinheim, Germany, 2007; p 255. (c) See also: Oestreich, M.; Rendler, S. *Synthesis* **2005**, 1727. (d) Orito, Y.; Nakajima, M. *Synthesis* **2006**, 1391. (e) Benaglia, M.; Guizzetti, S.; Pignataro, L. *Coord. Chem. Rev.* 2007, doi: 10.1016/j.ccr.2007.10.009.
(8) Short, J. D.; Attenoux, S.; Berrisford, D. J. *Tetrahedron Lett.* **1997**, *38*, 2351.
(9) Wang, Z.; Xu, G.; Wang, D.; Pierce, M. E.; Confalone, P. N. *Tetrahedron Lett.* **2000**, *41*, 4523.

Scheme 1. Allylation of Aldehydes **1** with Allyl and Crotyl Trichlorosilanes **2–4**[a]

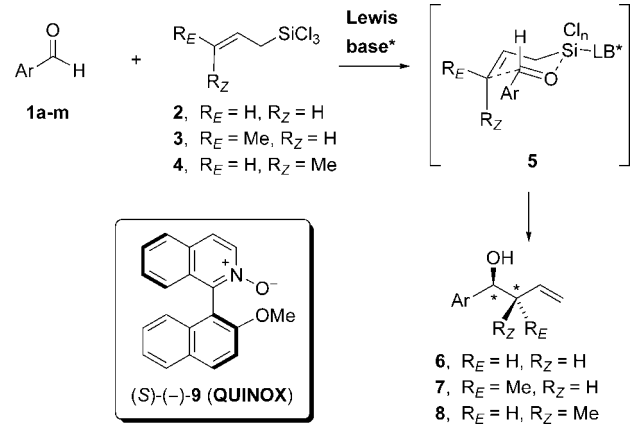

[a] For **a**−**m**, see Table 1.

Chart 1. Selected Lewis Basic Catalysts for Allylation of Aldehydes with **2a**

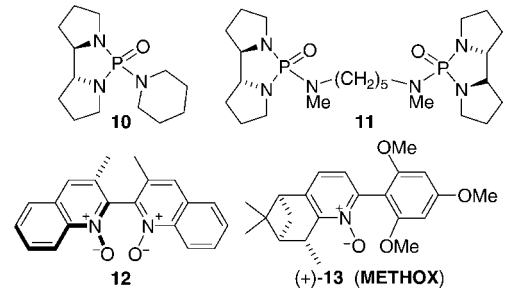

their Si and Sn counterparts and do not require an activator.[13] Similarly, the chelates, generated from allyltrichlorosilane and a stoichiometric amount of an amino alcohol, such as pseudoephedrine, do not require further activation and have been shown to produce the corresponding homoallylic alcohols **6** with high enantioselectivity.[14]

Asymmetric allylation of aldehydes **1** with allyl- and crotyltrichlorosilanes **2**-**4**, catalyzed by chiral Lewis bases (Scheme 1), in particular phosphoramides **10** and **11**,[15–17] bipyridine *N,N*-bisoxides (e.g., **12**),[18–20] and terpyridine *N,N,N*-trisoxides[21] (Chart 1) has evolved into an efficient method for the synthesis of enantiomerically enriched homoallylic alcohols **6**−**8** (Scheme 1).[1,7] In general, the reaction displays an excellent diastereocontrol in the case of *trans*- and *cis*-crotylsilanes (**3**/**4**), suggesting the cyclic transition state (TS) **5**. In a detailed investigation into the mechanism of allylation catalyzed by chiral phosphoramides, Denmark has found that the reaction follows a first order kinetics in both silane and aldehyde and a second order in the monodentate phosphoramide promoter (**10**).[16a,22,23] Hence, not surprisingly, bidentate Lewis bases, such as bisphosphoramides (**11**)[16a,22] and bipyridine *N,N′*-dioxides (**12**),[18,19] proved to be superior in reactivity and selectivity compared to monodentate catalysts.[7]

In parallel, we have introduced a family of chiral pyridine *N*-monooxides, such as **9** (QUINOX) and **13** (METHOX), acting as remarkably efficient monodentate catalysts in the allylation reaction (Scheme 1) with up to 98% ee.[24,25] In a preliminary communication,[25] we have demonstrated that, despite the structural similarity across the whole series, QUINOX (**9**) displayed an unusual reactivity pattern, for which a mechanistic rationale is presented herein.

Results and Discussion

In the past few years, we have developed a series of chiral pyridine *N*-oxide organocatalysts for the enantioselective allylation of aromatic aldehydes **1** with allyltrichlorosilanes **2**–**4**

(10) (a) Iseki, K.; Mizuno, S.; Kuroki, Y.; Kobayashi, Y. *Tetrahedron Lett.* **1998**, *39*, 2767. (b) Iseki, K.; Mizuno, S.; Kuroki, Y.; Kobayashi, Y. *Tetrahedron* **1999**, *55*, 977. (c) For analogous activation of Cl_3SiH by chiral tertiary amides derived from amino acids, see: Iwasaki, F.; Omonura, O.; Mishima, K.; Kanematsu, T.; Maki, T.; Matsumura, Y. *Tetrahedron Lett.* **2001**, *42*, 2525. (d) Malkov, A. V.; Mariani, A.; MacDougall, K. N.; Kočovský, P. *Org. Lett.* **2004**, *6*, 2253.
(11) (a) Kobayashi, S.; Nishio, K. *Chem. Lett.* **1994**, 1773. (b) Kobayashi, S.; Nishio, K. *J. Org. Chem.* **1994**, *59*, 6620. (c) Kobayashi, S.; Nishio, K. *J. Org. Chem.* **1994**, *59*, 6620.
(12) Chataigner, I.; Piarulli, U.; Gennari, C. *Tetrahedron Lett.* **1999**, *40*, 3633.
(13) (a) Smith, K. In *Organometallics in Synthesis*; Schlosser, M., Ed.; J. Wiley and Sons; Chichester, U.K., 2002; p 514. (b) Chemler, S. R.; Roush, W. R. In *Modern Carbonyl Chemistry*; Otera, J., Ed.; Wiley-VCH: Weinheim, 2000; Chapter 11.
(14) (a) Wang, X.; Meng, Q.; Nation, A. J.; Leighton, J. L. *J. Am. Chem. Soc.* **2002**, *124*, 10672. (b) Kinnaird, J. W. A.; Ng, P. Y.; Kubota, K.; Wang, X.; Leighton, J. L. *J. Am. Chem. Soc.* **2002**, *124*, 7920. (c) Kubota, K.; Leighton, J. L. *Angew. Chem., Int. Ed.* **2003**, *42*, 946.
(15) (a) Iseki, K.; Kuroki, Y.; Takahashi, M.; Kishimoto, S.; Kobayashi, Y. *Tetrahedron* **1997**, *53*, 3513. (b) Wadamoto, M.; Ozasa, N.; Yanagisawa, A.; Yamamoto, H. *J. Org. Chem.* **2003**, *63*, 5593. (c) Iseki, K.; Kuroki, Y.; Takahashi, M.; Kobayashi, Y. *Tetrahedron Lett.* **1996**, *37*, 5149.
(16) (a) Denmark, S. E.; Fu, J. *J. Am. Chem. Soc.* **2000**, *122*, 12021. (b) Denmark, S. E.; Fu, J. *J. Am. Chem. Soc.* **2001**, *123*, 9488.
(17) Hellwig, J.; Belser, T.; Müller, J. F. K. *Tetrahedron Lett.* **2001**, *42*, 5417.
(18) (a) Nakajima, M.; Saito, M.; Shiro, M.; Hashimoto, S. *J. Am. Chem. Soc.* **1998**, *120*, 6419. (b) Nakajima, M.; Saito, M.; Hashimoto, S. *Chem. Pharm. Bull.* **2000**, *48*, 306.
(19) (a) Shimada, T.; Kina, A.; Ikeda, S.; Hayashi, T. *Org. Lett.* **2002**, *4*, 2799. (b) Shimada, T.; Kina, A.; Hayashi, T. *J. Org. Chem.* **2003**, *68*, 6329. (c) Kina, A.; Shimada, T.; Hayashi, T. *Adv. Synth. Catal.* **2004**, *346*, 1169.
(20) (a) For reviews, see : Chelucci, G.; Thummel, R. P. *Chem. Rev.* **2002**, *102*, 3129. (b) Malkov, A. V.; Kočovský, P. *Curr. Org. Chem.* **2003**, *7*, 1737. (c) Chelucci, G.; Murineddu, G.; Pinna, G. A. *Tetrahedron: Asymmetry* **2004**, *15*, 1373. (d) Kwong, H. L.; Yeung, H. L.; Yeung, C. T.; Lee, W. S.; Lee, C. S.; Wong, W. L. *Coord. Chem. Rev.* **2007**, *251*, 2188. (e) For the most recent example of bipyridine *N,N*-bisoxide catalyst, see : Chelucci, G.; Belmonte, N.; Benaglia, M.; Pignataro, L. *Tetrahedron Lett.* **2007**, *48*, 4037.
(21) Wong, W.-L.; Lee, C.-S.; Leung, H.-K.; Kwong, H.-L. *Org. Biomol. Chem* **2004**, *2*, 1967.
(22) (a) Denmark, S. E.; Fu, J.; Coe, D. M.; Su, X.; Pratt, N. E.; Griedel, B. D. *J. Org. Chem.* **2006**, *71*, 1513. (b) For mechanistic studies on the related aldol reaction, see: Denmark, S. E.; Bui, T. *Proc. Natl. Acad. Sci. U.S.A.* **2004**, *101*, 5439. (c) Denmark, S. E.; Bui, T. *J. Org. Chem.* **2005**, *70*, 10393. (d) Denmark, S. E.; Pham, S. M.; Stavenger, R. A.; Su, X.; Wong, K.-T.; Nishigaichi, Y. *J. Org. Chem.* **2006**, *71*, 3904. (e) For mechanistic studies on Lewis-base catalyzed opening of epoxides with chlorosilanes, see: Denmark, S. E.; Barsanti, P. A.; Beutner, G. L.; Wilson, T. W. *Adv. Synth. Catal.* **2007**, *349*, 567.
(23) In the allylation, unlike in the related aldol reaction (ref 22d), the minor, one catalyst manifold could not be characterized (ref 22a).
(24) (a) Malkov, A. V.; Orsini, M.; Pernazza, D.; Muir, K. W.; Langer, V.; Meghani, P.; Kočovský, P. *Org. Lett.* **2002**, *4*, 1047. (b) Malkov, A. V.; Bell, M.; Orsini, M.; Pernazza, D.; Massa, A.; Herrmann, P.; Meghani, P.; Kočovský, P. *J. Org. Chem.* **2003**, *68*, 9659. (c) Malkov, A. V.; Bell, M.; Vassieu, M.; Bugatti, V.; Kočovský, P. *J. Mol. Catal. A* **2003**, *196*, 179. (d) Malkov, A. V.; Bell, M.; Castelluzzo, F.; Kočovský, P. *Org. Lett.* **2005**, *7*, 3219. (e) For other *N*-monooxide catalysts, see: Traverse, J. F.; Zhao, Y.; Hoveyda, A. H.; Snapper, M. L. *Org. Lett.* **2005**, *7*, 3151. (f) Chai, Q.; Song, C.; Sun, Z.; Ma, Y.; Ma, C.; Dai, Y.; Andrus, M. B. *Tetrahedron Lett.* **2006**, *47*, 8611. (g) Pignataro, L.; Benaglia, M.; Annunziata, R.; Cinquini, M.; Cozzi, F. *J. Org. Chem.* **2006**, *71*, 1458.
(25) Malkov, A. V.; Dufková, L.; Farrugia, L.; Kočovský, P. *Angew. Chem., Int. Ed.* **2003**, *42*, 3674.

Scheme 2. Synthesis of QUINOX and its Deoxy Analogue

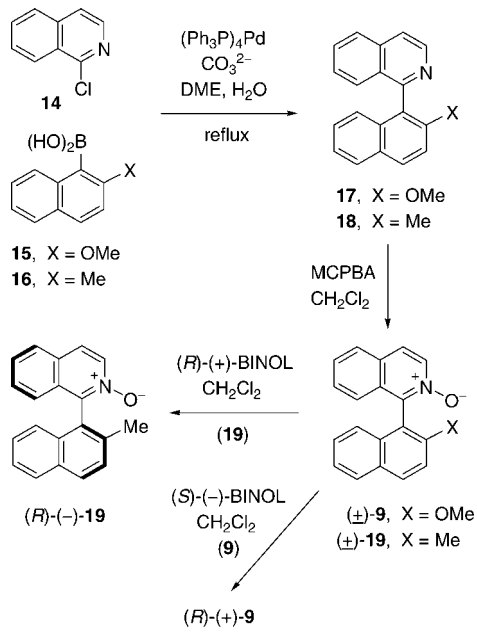

(Scheme 1). Thus, for instance, the terpene-derived METHOX (**13**) and its congeners have been shown by us to work generally very well and to tolerate a wide range of electron-poor and electron-rich benzaldehydes, exhibiting little dependence of the reaction rate and enantioselectivity on the nature of the Ar group in **1** (96 and 93% ee for 4-$MeOC_6H_4CHO$ and 4-$CF_3C_6H_4CHO$, respectively, with **13** as catalyst).[24d] However, in contrast to most of the catalysts reported to date, QUINOX (**9**), another member of the *N*-oxide family, exhibited a significant preference toward electron-poor aldehydes (96% ee with 4-$CF_3C_6H_4CHO$), whereas electron-rich substrates reacted much slower and were characterized by dramatically lower selectivities (16% ee for 4-$MeOC_6H_4CHO$!).[25] This intriguing behavior suggests that two fundamentally different mechanisms operate in these reactions as a function of the catalyst structure, which prompted us to embark on a detailed mechanistic study.

Synthesis of QUINOX (9) and its Methyl Analogue (19). The synthesis of QUINOX **9**, briefly described in our preliminary communication (Scheme 2),[25,26] was inspired by the initial steps toward QUINAP.[27] Thus, the Suzuki−Miyaura coupling of 1-chloro-isoquinoline (**14**)[27b] with boronic acid **15**,[27b,28] carried out in refluxing DME in the presence of Cs_2CO_3 and $(Ph_3P)_4Pd$ (3 mol%) overnight, afforded the biaryl derivative **17**[27] (95%), whose treatment with *m*-chloroperoxybenzoic acid provided the racemic *N*-oxide (±)-**9** (99%). The latter racemate was resolved by cocrystallization with (*S*)-(−)-2,2′-dihydroxy-1,1′-binaphthyl (BINOL),[29] which gave the crystalline material containing (*S*)-(−)-BINOL and (+)-**9** in a 1:1 ratio, while (−)-**9** remained in the solution. This cocrystallization, followed by a chromatographic separation of (+)-**9** from (*S*)-BINOL, furnished pure (+)-**9** of 98% ee (as revealed by chiral HPLC) in 89% isolated yield.[26] The absolute configuration of **9** was found to be (*R*)-(+)-**9** by crystallographic analysis of the molecular crystal of (*S*)-(−)-BINOL•(+)-**9** (Figure 1A).[25]

To asses the electronic role of the methoxy group in QUINOX (**9**), we have now synthesized its methyl analogue **19** (Scheme 2). The synthesis was carried out in the same way as that of QUINOX, namely, via the Suzuki−Miyaura coupling of 1-chloro-isoquinoline (**14**)[27b] with boronic acid **16**, which in turn was prepared from 1-bromo-2-methyl naphthalene by lithiation with *n*-BuLi in THF, followed by a reaction with $(MeO)_3B$ and subsequent hydrolysis of the intermediate boronate ester with HCl.[25,27b,30] The coupling itself was carried out by refluxing a mixture of **14** and **16** in DME with aqueous K_2CO_3 and $(Ph_3P)_4Pd$ as catalyst (3 mol %) for 48 h to afford **18** (71%). Oxidation of the latter derivative with MCPBA gave rise to the racemic *N*-oxide **19** (81%), which was resolved by cocrystallization with (*R*)-(+)-BINOL from CH_2Cl_2.[29] The crystals contained the molecular compound (*R*)-BINOL•(*R*)-**19**, as revealed by single crystal X-ray analysis (Figure 1B). Flash chromatography of the latter material gave (*R*)-(−)-**19** (33%; ≥99.5% ee) and the recovered (*R*)-(+)-BINOL. The mother liquor provided the enantiomerically enriched (*S*)-**19**, which was purified by cocrystallization with (*S*)-(−)-BINOL to produce (*S*)-(+)-**19** (19%; ≥99.8% ee).

Allylation of Aldehydes 1a−m Catalyzed by QUINOX (9). Addition of allyltrichlorosilane (**2**) to benzaldehyde (**1a**) (Scheme 1), carried out in the presence of (*R*)-(+)-**9** (5 mol %) at −40 °C for 12 h, produced (*R*)-(+)-**6a** of 87% ee (Table 1, entry 1). Lowering the catalyst load to 1 mol % slowed the reaction but had no effect on the enantioselectivity (entry 2).

The solvent effect was investigated briefly. In MeCN, the reaction was slower and rather less enantioselective than that in CH_2Cl_2 (compare entries 1 and 5). Further decrease of enantioselectivity was observed for $CHCl_3$ (63% ee, entry 6), but the reaction proved to be much faster (30 min at −40 °C). On the other hand, in toluene, the reaction became very sluggish owing to poor solubility of the catalyst (entry 7), although moderate asymmetric induction (61% ee) was still observed.

Introduction of electron-withdrawing substituents into the aromatic ring of the aldehyde resulted in a notable increase in both reactivity and enantioselectivity. Thus, *p*-nitrobenzaldehyde **1b** afforded the corresponding product in better yield and with slightly higher ee than benzaldehyde (compare entries 1 and 8); the halo derivatives **1c−f** gave >90% ee (entries 9–12). The highest conversion and enantioselectivity (96% ee) was attained with the *p*-trifluoromethyl derivative **1g** (entry 13).

By contrast, the electron-rich *p*-methoxybenzaldehyde (**1h**) afforded an almost racemic product (entry 16) and its *o*-isomer **1i** also showed low selectivity (entry 19); deceleration was observed in both cases. On the other hand, *m*-methoxybenzaldehyde **1j** (entry 20), where the methoxy group serves as a weak acceptor, again showed a good level of selectivity (80% ee), although the reaction was still quite slow. 3,5-Dimethylbenzal-

(26) (+)-QUINOX has been first prepared by Nakajima, including the same Suzuki−Miyaura coupling and resolution. However, the synthesis was mentioned as a footnote without revealing the conditions, and the absolute configuration was not determined. Nakajima, M.; Saito, M.; Uemura, M.; Hashimoto, S. *Tetrahedron Lett.* **2002**, *43*, 8827.

(27) (a) Brown, J. M.; Hulmes, D. I.; Layzell, T. P. *J. Chem. Soc., Chem. Commun.* **1993**, 1673. (b) Alcock, N. W.; Brown, J. M.; Hulmes, D. I. *Tetrahedron: Asymmetry* **1993**, *4*, 743.

(28) Vyskočil, Š.; Meca, L.; Tišlerová, I.; Císařová, I.; Polášek, M.; Harutyunyan, S. R.; Belokon, Y. N.; Stead, R. M. J.; Farrugia, L.; Lockhart, S. C.; Mitchell, W. L.; Kočovský, P. *Chem. Eur. J.* **2002**, *8*, 4633.

(29) For the previous use of BINOL as a resolving agent, see refs 18, 19a, 26, and Nakajima, M.; Saito, M.; Hashimoto, S. *Tetrahedron: Asymmetry* **2002**, *13*, 2449.

(30) Pathak, R.; Nhlapo, J. M.; Govender, S.; Michael, J. P.; van Otterlo, W. A. L.; de Koning, C. B. *Tetrahedron* **2006**, *62*, 2820.

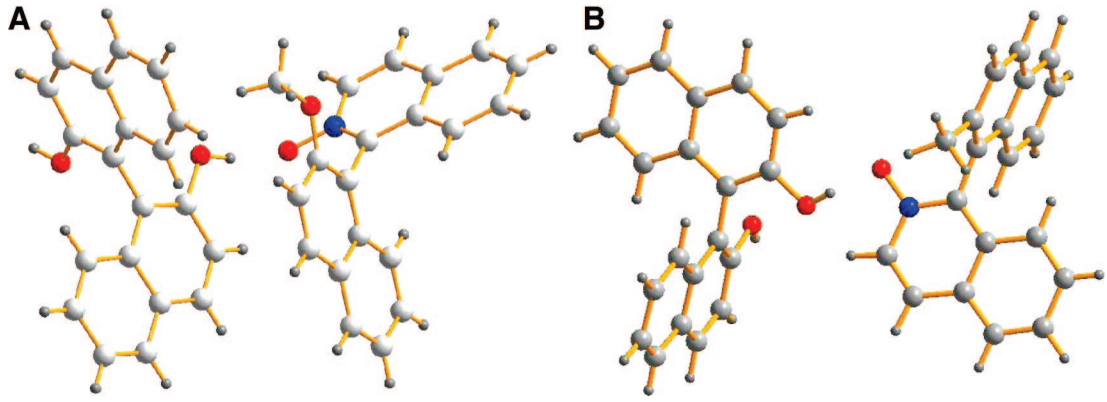

Figure 1. (A) Disposition of the molecules in the crystal containing (*R*)-(+)-**9** (right) and (*S*)-(−)-BINOL (left) as shown by X-ray crystallography. (B) Molecules in the crystal of (*R*)-(−)-**19** (right) with (*R*)-(+)-BINOL (left). Both diagrams illustrate the N−O···H−O hydrogen bonding.

Table 1. The Allylation of Aldehydes **1a-m** with Allylsilane **2**, Catalyzed by **9** and **19** (Scheme 1)[a]

entry	catalyst	aldehyde	Ar	solvent	time (h)	t (°C)	yield (%)[b]	ee (%)[c,d]
1	(*R*)-(+)-**9**	**1a**	Ph	CH_2Cl_2	12	−40	68	87 (*R*)
2	(*R*)-(+)-**9**[e]	**1a**	Ph	CH_2Cl_2	12	−40	55	87 (*R*)
3	(*R*)-(+)-**9**	**1a**	Ph	CH_2Cl_2	12	−20	76	84 (*R*)
4	(*R*)-(+)-**9**	**1a**	Ph	CH_2Cl_2	2	18	40	65 (*R*)
5	(*R*)-(+)-**9**	**1a**	Ph	MeCN	12	−40	60	72 (*R*)
6	(*R*)-(+)-**9**	**1a**	Ph	$CHCl_3$	0.5	−40	79	63 (*R*)
7	(*R*)-(+)-**9**	**1a**	Ph	toluene	12	−40	<5	61 (*R*)
8	(*R*)-(+)-**9**	**1b**	4-NO_2−C_6H_4	CH_2Cl_2	2	−40	73	89 (*R*)
9	(*R*)-(+)-**9**	**1c**	4-Cl−C_6H_4	CH_2Cl_2	2	−40	65	93 (*R*)
10	(*R*)-(+)-**9**	**1d**	2-Cl−C_6H_4	CH_2Cl_2	2	−40	72	91 (*R*)
11	(*R*)-(+)-**9**	**1e**	3-Cl−C_6H_4	CH_2Cl_2	2	−40	49	95 (*R*)
12	(*R*)-(+)-**9**	**1f**	4-F−C_6H_4	CH_2Cl_2	2	−40	79	91 (*R*)
13	(*R*)-(+)-**9**	**1g**	4-CF_3−C_6H_4	CH_2Cl_2	2	−40	85	96 (*R*)
14	(*R*)-(+)-**9**	**1g**	4-CF_3−C_6H_4	CH_2Cl_2	2	−20	88	91 (*R*)
15	(*R*)-(+)-**9**	**1g**	4-CF_3−C_6H_4	CH_2Cl_2	2	0	65	89 (*R*)
16	(*S*)-(−)-**9**	**1h**	4-MeO−C_6H_4	CH_2Cl_2	18	−40	70	16 (*S*)[f]
17	(*S*)-(−)-**9**	**1h**	4-MeO−C_6H_4	CH_2Cl_2	18	−20	45	72 (*S*)[f]
18	(*S*)-(−)-**9**	**1h**	4-MeO−C_6H_4	CH_2Cl_2	18	0	10	45 (*S*)[f]
19	(*R*)-(+)-**9**	**1i**	2-MeO−C_6H_4	CH_2Cl_2	12	−40	73	37 (*R*)
20	(*R*)-(+)-**9**	**1j**	3-MeO−C_6H_4	CH_2Cl_2	12	−40	40	80 (*R*)
21	(*R*)-(+)-**9**	**1k**	3,5-$Me-C_6H_3$	CH_2Cl_2	16	−40	68	81 (*R*)
22	(*R*)-(+)-**9**	**1l**	PhCH=CH	CH_2Cl_2	12	−40	86	51 (*R*)
23	(*R*)-(+)-**9**	**1m**	PhCH=C(Me)	CH_2Cl_2	12	−40	71	55 (*R*)
24	(*R*)-(−)-**19**[g]	**1a**	Ph	CH_2Cl_2	12	−40	19	64 (*S*)
25	(*R*)-(−)-**19**[g]	**1g**	4-CF_3−C_6H_4	CH_2Cl_2	12	−40	26	71 (*S*)
26	(*R*)-(−)-**19**[g]	**1h**	4-MeO−C_6H_4	CH_2Cl_2	12	−40	7	7 (*S*)

[a] The reaction was carried out at 0.4 mmol scale with 1.1 equiv of **2**, in the presence of **9** (5 mol %, ≥98% ee) or **19** (5 mol %, ≥99% ee) as catalyst, and (*i*-Pr)$_2$NEt (1 equiv) as base, unless stated otherwise. [b] Isolated yield. [c] Determined by chiral HPLC or GC. [d] The configuration of the products **6** was established by the comparison of their optical rotations (measured in $CHCl_3$) and their GC and HPLC retention times with the literature data and with the behavior of authentic samples (refs 24 and 25). [e] With 1 mol % of the catalyst. [f] Note that this experiment was carried out with (*S*)-(−)-**9**. [g] Note that because of the change of substituent preferences in the CIP nomenclature, (*R*)-**19** actually corresponds to (*S*)-**9**.

dehyde **1k** exhibited good reactivity and enantioslelectivity (entry 21), while cinnamyl derivatives **1l** and **1m** produced modest results (entries 22 and 23).

Investigation of the effects of temperature on the enantioselectivity of allylation catalyzed by QUINOX (**9**) revealed that benzaldehyde **1a** and its electron poor *p*-trifluoromethyl derivative **1g** behaved in an ordinary fashion, showing a slight erosion of the ee at increased temperatures (entries 1, 3, and 4 for **1a** and 13–15 for **1g**). At the same time, the electron-rich *p*-methoxybenzaldehyde **1h** exhibited a significant temperature dependence (entries 16–18), known as isoinversion effect,[31] where the highest value of 72% ee was achieved at −20 °C. Furthermore, the increase in temperature had a significant deceleration effect in the case of **1h** (entries 16–18), reflected in a decreased yield (and an increased amount of the unreacted aldehyde recovered).

Allylation Catalyzed by Methyl−QUINOX (19). The reactivity of the *N*-oxide **19**, a methyl analogue of QUINOX, was explored with the aid of three representative aldehydes **1a**,**g**,**h** (Table 1, entries 24–26). Compared to QUINOX, the reactions turned out to be much slower and the enantioselectivities lower. Nevertheless, the same trend was observed, that is, the electron-poor **1g** was the most reactive of the series, while the worst results were obtained with the electron-rich aldehyde **1h**. This behavior clearly shows that the methoxy group in QUINOX (**9**) not only serves as steric element preventing the rotation about the chiral axis but also must play an additional, presumably electronic, role.

(31) (a) For a discussion of isoinversion principle, see: Schmid, R.; Sapunov, V. N. *Non-formal Kinetics*; VCH: Weinheim, Germany, 1982. (b) Gypser, A.; Norrby, P.-O. *J. Chem. Soc. Perkin Trans. 2* **1997**, 939.

Table 2. The Allylation of Aldehydes **1a**,**g**,**h** with Allylsilanes **3** (*E*/*Z* ≥ 98:2) and **4** (*E*/*Z* ≤ 2:98) Catalyzed by (*S*)-(−)-**9** (Scheme 1)[a]

entry	aldehyde	Ar	silane	yield %[b]	**7**:**8** (anti:syn)	% ee (configuration)[c,d] anti, syn
1	**1g**	4-CF_3−C_6H_4	**3**	75	96:4	92 (1*S*,2*S*), 90 (1*S*,2*R*)
2	**1a**	Ph	**3**	65	95:5	66 (1*S*,2*S*), 77 (1*S*,2*R*)
3	**1h**	4-MeO-C_6H_4	**3**	40	83:17	25 (1*S*,2*S*), 12 (1*R*,2*S*)
4	**1g**	4-CF_3−C_6H_4	**4**	85	1:99	nd, 94 (1*S*,2*R*)
5	**1a**	Ph	**4**	78	1:99	69 (1*S*,2*S*), 79 (1*S*,2*R*)
6	**1h**	4-MeO-C_6H_4	**4**	50	4:96	40 (1*R*,2*R*), 60 (1*S*,2*R*)

[a] The reaction was carried out at 0.4 mmol scale with 1.1 equiv of **3**/**4**, in the presence of (*S*)-(−)-**9** (5 mol %, 98% ee) as catalyst and (*i*-Pr)$_2$NEt (1 equiv) as base in CH_2Cl_2 at –40 °C for 24 h. [b] Isolated yield. [c] Determined by chiral GC. [d] The absolute configuration of **7**/**8** was determined by comparison of their optical rotations (measured in $CHCl_3$) and their GC retention times with the literature data (refs 16b, 33) and with the behavior of authentic samples.

Crotylation Catalyzed by QUINOX (9). The crotylation reaction was found by us to be highly diastereoselective,[25] which is consistent with the cyclic chairlike transition state **5**. Previously, we reported that addition of crotyltrichlorosilane **3** (trans/cis ratio 87:13) to benzaldehyde (**1a**), catalyzed by QUINOX (**9**), produced a ∼70:30 mixture of **7a** and **8a**, suggesting a partial loss of diastereoselectivity.[25] We have now repeated these experiments with the isomerically pure **3** (trans/cis ≥ 98:2)[32] and **4** (trans/cis ≤ 2:98)[32] and found that the reaction, in fact, was highly diastereoselective for both **1a** and **1g** (Table 2, entries 1, 2, 4, and 5);[33] only with the electron-rich **1h** (entries 3 and 6) it was less stereoconvergent. Significantly, *cis*-crotylsilane **4** exhibited a higher rate of allylation compared to the trans isomer **3**, which represents a reversal of the trend commonly observed with other *N*-oxide catalysts,[24] in particular METHOX (**13**).[24d] On the basis of these results, the seeming loss of diastereocontrol, reported by us previously for **3** with the 87:13 trans/cis ratio,[25] can now be attributed to a higher reactivity of the minor cis isomer **4**, thus showing a kinetic preference of QUINOX (**9**) toward *cis*-crotylsilane (in the excess of the geometrically impure reagent). Erosion of diastereoselectivity in the case of **1h** was accompanied by low enantioselectivities (entries 3 and 6). Furthermore, the absolute configuration at C(1) of the minor product proved to be opposite to that of the major diastereoisomer (entries 3 and 6), demonstrating an inversion of the facial attack at the C═O bond from *si* to *re*, which may originate from participation of a twisted boatlike transition structure.[34]

A probe into the possible nonlinear effect in the allylation of **1a** with **2**, catalyzed by (*R*)-(+)-**9** of 29%, 50%, and 75% ee, respectively, has demonstrated a fully linear relationship between the enantiopurity of the catalyst and the product. In these experiments, the resulting alcohol **6a** was of 27%, 45%, and 71% ee, respectively.

Kinetic Experiments. To shed light on the mechanism, a series of kinetic experiments were carried out. The order in each component was determined by using the method of initial rates. A sampling technique was employed, in which the aliquots taken at certain intervals were analyzed by GC to monitor the product formation. Although the high sensitivity of the reaction to traces of moisture complicated the data collection, acceptable reproducibility was achieved up to the 20% conversion. The reaction followed a first-order kinetics in aldehyde (1.12 for **1g**), whereas the order in silane exhibited an unusual behavior, irrespective of the nature of the aldehyde. The lg/lg plot of the initial rates

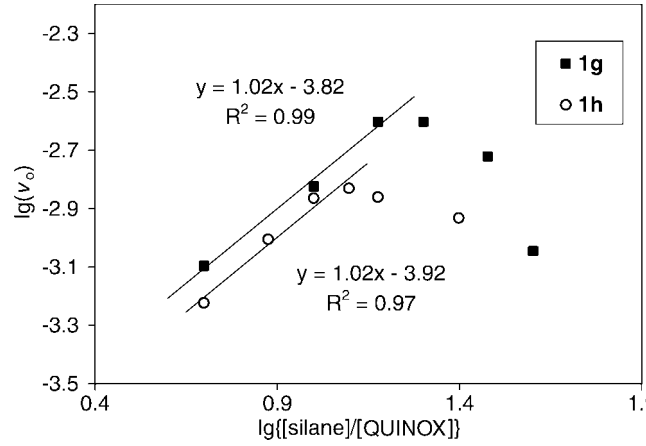

Figure 2. Reaction order in **2**.

(v_o) versus the [silane]/[catalyst] ratio (Figure 2) consists of two distinct areas. At the silane/catalyst ratio up to 15:1 (lg value 1.18), the order in silane is unity (1.02 for both **1g** and **1h**), whereas above that point the reaction slows down and the order in silane turns negative.[35] At low silane-to-catalyst ratios, the kinetic data obtained for aldehyde **1g** and silane **2** mirror those reported by Denmark for phosphoramides.[16a,22] However, the order in QUINOX (**9**), determined at 10–25 mol % loadings (with 1 equiv of **1g** and 1.5 equiv of **2**), was found close to unity (0.82), which contrasts with the second order observed for monodentate phosphoramides. Taking into account the reversible nature of the coordination of QUINOX (**9**) to silane **2** and the absence of a nonlinear effect (in the case of **9**), combined with the observations that enantioselectivity is not affected by catalyst loading in the range of 1–10 mol %,[25] it appears very likely that only one molecule of the catalyst is involved in the rate and selectivity determining step.

The rate limiting step (RLS) was elucidated by using Hammett correlation. The plot in Figure 3 shows that electron-withdrawing substituents accelerated the reaction ($\rho = 1.18$), indicating that it is the electrophilicity of the carbonyl carbon (rather than the Lewis basicity of the carbonyl oxygen) that influences the reactivity. This observation is consistent with the rate determining C−C bond formation rather than pre-equilibration.[36] This ρ value also suggests that the reaction center in the

(32) Iseki, K.; Kuroki, Y.; Takahashi, M.; Kishimoto, S.; Kobayashi, Y. *Tetrahedron* **1997**, *53*, 3513.
(33) (a) For comparison, see ref 16b and the following: Hackman, B. M.; Lombardi, P. J.; Leighton, J. L. *Org. Lett.* **2004**, *6*, 4375. (b) McManus, H. A.; Cozzi, P. G.; Guiry, P. J. *Adv. Synth. Catal.* **2006**, *348*, 551.
(34) For a similar effect in the related aldol reaction, ref 22d.
(35) Analysis of the reaction mixtures by ^{1}H NMR revealed that both catalysts **9** and **19** remained intact for the duration of the process; no reduction of the *N*-oxide group or catalyst decomposition was observed under the reaction conditions.
(36) In the allylation, the C−C bond formation was assumed to be a rate-limiting step (ref 22a) but not confirmed by kinetic experiments.

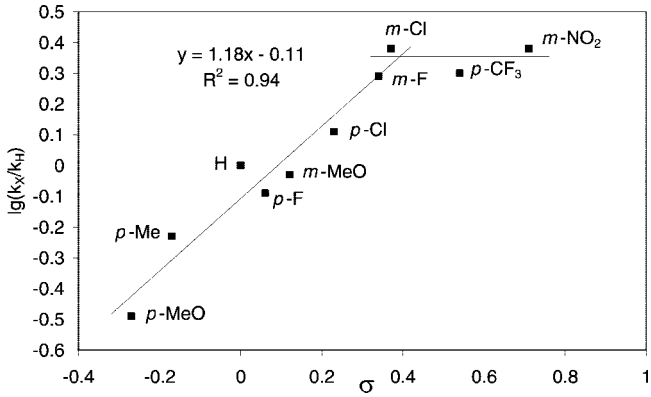

Figure 3. Hammett plot for the allylation of **1** with **2** catalyzed by **9**.

Scheme 3. Allylation of Benzaldehyde **1a** Catalyzed by QUINOX (**9**)

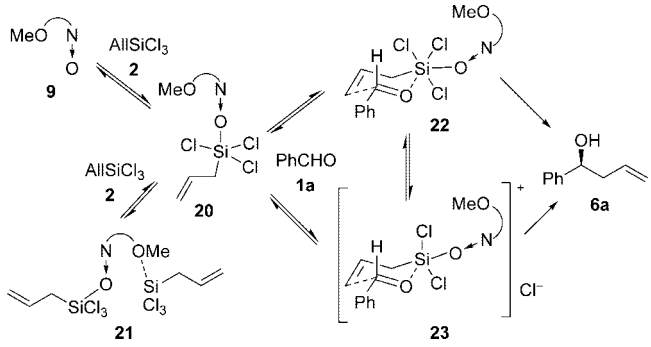

TS is nonionic, weakly polar,[37] implying that the Lewis acidity of the silicon in **5** is just sufficient to allow binding of aromatic aldehydes but without affecting their electrophilicity. At higher σ values, deviation from linearity was observed,[38,39] indicating a gradual shift in the RLS toward precoordination. These data were corroborated by the measurement of the secondary isotope effect (SIE), namely by comparing the relative reactivities of ArCD═O vs ArCH═O. In the case of **1h**, the SIE value of 0.70 indicates a late transition state, closely resembling the sp^3 hybridized product. The sp^2-character in the TS gradually increased as evidenced by the increase in the SIE to 0.81 (for **1a**) and further to 0.86 (for **1g**), confirming a shift toward precoordination RLS, which is reflected in the first order kinetics in **1g**.

On the basis of the kinetic data, the following mechanistic scenario can be proposed (Scheme 3). Allyltrichlorosilane (**2**) and QUINOX (**9**) reversibly form the reactive complex **20**, which is deactivated by a large excess of the silane, presumably via binding a second molecule of **2** to generate a catalytically inactive complex, such as **21** (vide infra). The negative order in silane **2** at higher concentrations arises from the need to release the extra silane molecule to return to **20**. The next reaction step, binding the aldehyde, can proceed via associative (**22**) or dissociative (**23**) mechanisms.[22a] Since the octahedral complex **22** is more crowded than the trigonal bipyramidal **23**, participation of the tightly packed transitions state **22** can be expected to lead to higher selectivities. The low ρ value, together with the observed higher reaction rates and better selectivities attained in nonpolar solvents, is consistent with the reaction pathway via the neutral, octahedral transition state **22**. The observed maximum on the plot of enantioselectivity versus reaction temperature in the case of *p*-methoxybenzaldehyde **1h** (the inversion effect) is indicative of either a temperature-dependent shift in the RLS (from C−C− bond formation to pre-equilibrium) or competition between different mechanism;[31] however, at this point the kinetic data do not provide a definite answer.

To obtain further insight into the deactivation of QUINOX (**9**) by a large excess of allyltrichlorosilane (**2**), for which coordination of Si to the MeO group could be suggested (**21** in Scheme 3), we have investigated the methyl catalyst **19**, where the latter interaction cannot exist. Indeed, in the allylation of *p*-trifluomethylbenzaldehyde (**1g**), increasing the silane/catalyst ratio from 10:1 to 50:1 (while the concentration of aldehyde **1g** was kept constant) resulted in the proportional (∼4-fold) increase in the reaction rate; that is, no catalyst deactivation was taking place. However, it is pertinent to note that at the silane/catalyst ratio 10:1, QUINOX (**9**) reacted nearly 3.5 times faster than its methyl analogue **19**. Hence, the MeO group of QUINOX can be regarded as the key feature to attain sufficient reaction rates and high enantioselectivities (with the exception of electron-rich aldehydes, such as **1h**).

Quantum Chemical Calculations

To get a better insight into the mechanism of the allylation catalyzed by QUINOX (**9**), a computational analysis of the reaction coordinate and the transition states (TS) was carried out using benzaldehydes **1a** and **1h** as model substrates.

Computational Details. All density functional theory (DFT) calculations were carried out using the program Turbomole 5.7.[40] The Perdew−Burke−Ernzerhof (PBE) functional[41] has been used throughout. The calculations were expedited by expanding the Coulomb integrals in an auxiliary basis set, the resolution-of-identity (RI-J) approximation.[42,43] All geometry optimizations were carried out using the 6-31G(d) basis set,[44] whereas the single point energies were recomputed using the TZVP basis set.[45] To account for the description of dispersion forces (which are not described by the currently used DFT functionals), the empirical dispersion parameters were added to both the energy and gradients during geometry optimization and the calculations of the single point energies [DFT(+D) method].[46,47] Here, default parameters[47] were used, except for the C_6 parameters for Si, where the values for P were used, and Cl, where we used the values of Neumann and Perrin.[48] This method has been shown to essentially yield the data with ∼1 kcal mol^{-1} acuracy in comparison with the reference CCSD(T) values.[47]

(37) A similar value (ρ = 1.18) has been reported for the allylation of aldehydes with allysiliconates: Hosomi, A.; Kohra, S.; Ogata, K.; Yanagi, T.; Tominaga, Y. *J. Org. Chem.* **1990**, *55*, 2415.
(38) For an analogous nonlinear behavior at high σ values, observed for the silicon-directed aldol condensation, see: Myers, A. G.; Widdowson, K. L.; Kukkola, P. J. *J. Am. Chem. Soc.* **1992**, *114*, 2765.
(39) The plot incorporating all the data points showed lower statistical significance of R^2 = 0.87.

(40) Ahlrichs, R.; Bär, M.; Häser, M.; Horn, H.; Kölmel, C. *Chem. Phys. Lett.* **1989**, *162*, 165.
(41) Perdew, J. P.; Burke, K.; Ernzerhof, M. *Phys. Rev. Lett.* **1996**, *77*, 3865.
(42) Eichkorn, K.; Treutler, O.; Öhm, H.; Häser, M.; Ahlrichs, R. *Chem. Phys. Lett.* **1995**, *240*, 283.
(43) Eichkorn, K.; Weigen, F.; Treutler, O.; Ahlrichs, R. *Theor. Chim. Acta* **1997**, *97*, 119.
(44) Hehre, W. J.; Radom, L.; Schleyer, P. I. v. R.; Pople, J. A. *Ab Initio Molecular Orbital Theory*; Wiley-Interscience: New York, 1986.
(45) Schäfer, A.; Huber, C.; Ahlrichs, R. *J. Chem. Phys.* **1994**, *100*, 5829.
(46) Grimme, S. *J. Comput. Chem.* **2004**, *25*, 1463.
(47) Jurečka, P.; Černý, J.; Hobza, P.; Salahub, D. *J. Comput. Chem.* **2007**, *28*, 555.
(48) Neumann, M. A.; Perrin, M. A. *J. Phys. Chem. B* **2005**, *109*, 15531.

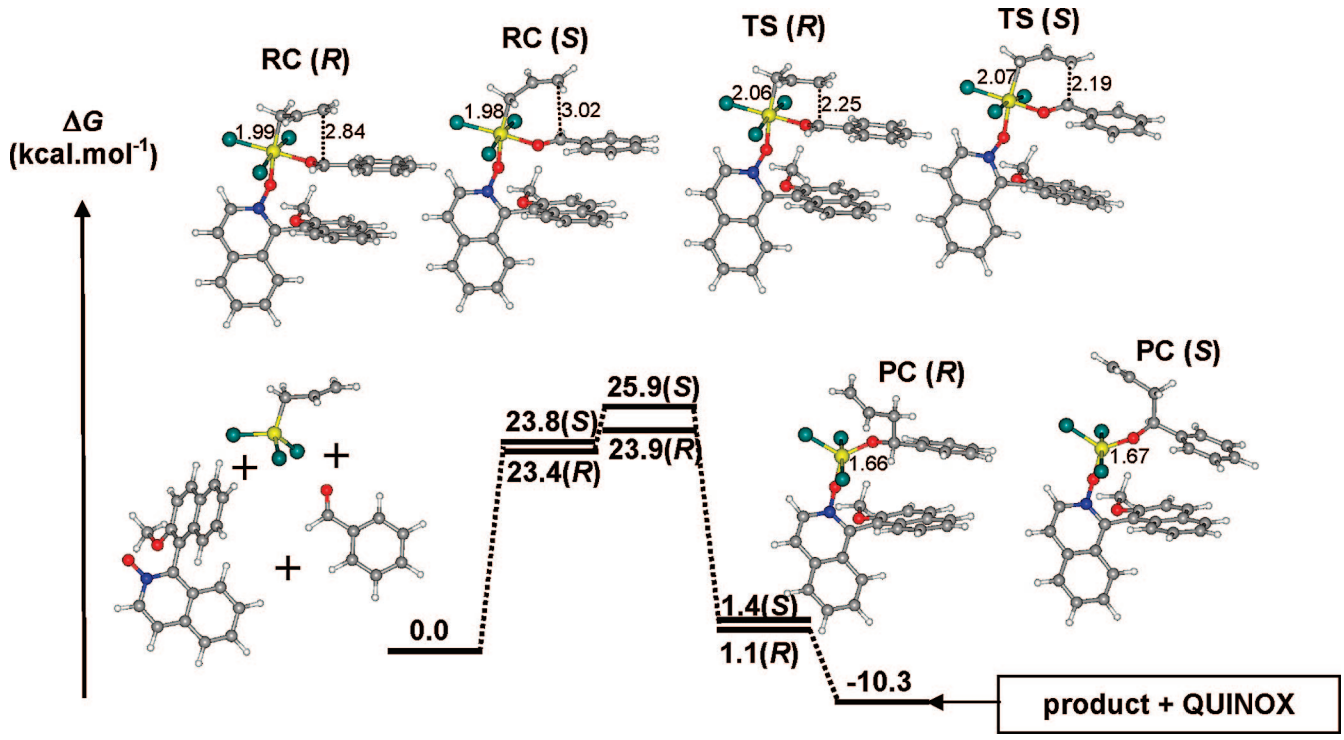

Figure 4. The equilibrium geometries of the most stable reactant complexes (RC), transition states (TS), and product complexes (PC) along the reaction coordinate for the associative pathway of allylation of benzaldehyde (**1a**) catalyzed by (*R*)-(+)-QUINOX (**9**). The calculated values for ΔG were obtained at the RI-PBE(+D)/TZVP//RI-PBE(+D)/6-31G(d) level; all distances are in Å.

To account for solvation effects, the conductor-like screening model (COSMO)[49,50] was employed with the dielectric constant corresponding to acetonitrile ($\epsilon_r = 36.6$). Gibbs free energy was then calculated as the sum of these contributions (equation 1):

$$G = E_{el(+D)} + G_{solv} + E_{ZPE} - RT\ln(q_{trans}q_{rot}q_{vib}) \qquad (1)$$

where $\Delta E_{el(+D)}$ is the in vacuo energy of the system [at the RI-PBE(+D)/TZVPP level, with the geometry optimized at the RI-PBE(+D)/6-31G(d) level (vide supra)], ΔG_{solv} is the solvation free energy [at the RI-PBE(+D)/6-31G(d) level] and the $E_{ZPE} - RT\ln(q_{trans}\, q_{rot}\, q_{vib})$ term is the zero-point energy, thermal corrections to the Gibbs free energy, and entropic term (obtained from a frequency calculation with the same method and software as for the geometry optimizations at the RI-PBE/6-31G(d) level, 298 K, and 1 atm pressure, using an ideal-gas approximation[51]).[52]

Transition state (TS) optimizations were performed as follows: First, the TS initial geometry was obtained by the constrained geometry optimization on the interpolated reaction coordinate, defined by the Si(1)−C(2) and C(4)−C(5) distances (Figure 4), which were assumed to attain the discrete values between the reactant and product with all the remaining internal coordinates optimized. The maximum on this approximate reaction coordinate was then taken as the initial guess for the saddle-point optimization along the eigenvector corresponding to the vibration with the imaginary frequency. Because of the lack of the analytic second derivatives in both DFT(+D) and COSMO solvation methods, the approximate method was used to obtain the transition states in solution: (1) the in vacuo optimization of transition state according to the above procedure; (2) constraining the Si(1)−C(2) and C(4)−C(5) distances to the values corresponding to the TS acquired in step 1 and optimizing all other degrees of freedom by the DFT(+D)/COSMO method. The difference between the DFT(+D)/COSMO energy at the in vacuo TS geometry and the relaxed geometry is denoted as the solvent relaxation term and is regarded to represent an accurate approximation to the true transition state in solution, calculated with the DFT(+D) method.

Finally, for benchmarking purposes on the model uncatalyzed reaction, the CCSD(T) method was used[53] with the aug-cc-pVDZ basis set.[54] These calculations were carried out using the MOLPRO program.[55,56]

Results of Computational Analysis

Approximately twenty structural variants for each of the reaction mechanisms using (*R*)-(+)-**9** were examined. Notably, the chelate arising by a bidentate coordination of QUINOX (**9**) to allyltrichlorosilane through the *N*-oxide and methoxy groups was found to be less stable by nearly 30 kcal mol^{-1} than the monocoordinated species **20**, which also rules out any contribution of the bidentate mode in the transition state.[57] The results covering the most stable structures are summarized in Table 3; the structures of the reactant and product complexes and transition states for the (*R*)- and (*S*)-reaction channels in the associative mechanism are shown in Figure 4. According to this analysis, the reaction commences with the formation of a

(49) Klamt, A.; Schuurmann, G. *J. Chem. Soc., Perkin Trans. 2* **1993**, 799.
(50) Schäfer, A.; Klamt, A.; Sattel, D.; Lohrenz, J. C. W.; Eckert, F. *Phys. Chem. Chem. Phys.* **2000**, *2*, 2187.
(51) Jensen, F. Introduction to Computational Chemistry; John Wiley & Sons: 1999.
(52) The free energy calculated according to equation 1 is regarded as a good approximation to ΔG in diluted solution.
(53) (a) Čížek, J. *J. Chem. Phys.* **1966**, *45*, 4256–4266. (b) Čížek, J. *Adv. Chem. Phys.* **1969**, *14*, 35–89. (c) Raghavachari, K.; Trucks, G. W.; Pople, J. A.; Head-Gordon, M. *Chem. Phys. Lett.* **1989**, *157*, 479.
(54) Woon, D. E.; Dunning, T. H., Jr. *J. Chem. Phys.* **1993**, *98*, 1358.
(55) Werner, H.-J.; et al. *MOLPRO*,. a package of ab initio programs, version 2002.6, 2006.
(56) Hampel, C.; Peterson, K.; Werner, H.-J. *Chem. Phys. Lett.* **1992**, *190*, 1.
(57) In fact, this value was obtained by constraining the complex geometry to preserve the bidentate binding mode of QUINOX, because this structure is not a minimum on the potential-energy surface of the complex and its geometry optimization converges to a monodentate structure.

Table 3. The Calculated Thermochemical Data for the Reaction of **1a** with **2** Catalyzed by (*R*)-(+)-QUINOX (**9**)[a]

entry	mechanism	product configuration	ΔG, reactant complex	$\Delta G^{\ddagger}$, transition state	ΔG, product complex
1	associative	*R*	23.4	23.9	1.1
2	associative	*S*	23.8	25.9	1.4
3	dissociative	*R*	19.3	26.0	1.1
4	dissociative	*S*	19.8	24.5	1.4

[a] All values are in kcal mol^{-1}.

transient reactant complex (RC). For the associative mechanism (**22**), this complex is higher in energy than the assembly of the isolated reactants and the catalyst by 23.4/23.8 kcal mol^{-1} (Table 3, entries 1 and 2) and for the dissociative mechanism (**23**) by 19.3/19.8 kcal mol^{-1} (entries 3 and 4); note the greater stability of the RC with cationic trigonal bipyramidal structure formed in the dissociative pathway. The calculated transition state barriers are $\Delta G^{\ddagger}_{\text{assoc}} = 23.9$ (*R*) and 25.9 (*S*) kcal mol^{-1}; and $\Delta G^{\ddagger}_{\text{dissoc}} = 26.0$ (*R*) and 24.5 (*S*) kcal mol^{-1} for the associative and dissociative mechanism, respectively.[58] Significantly, a narrow energy gap between the RC and TS in the associative mechanism correlates well with the experimentally observed borderline position of the RLS between precoordination of the substrate aldehyde and C−C bond formation. The overall reaction thermodynamics, after the catalyst has dissociated from the product complex (PC), is $\Delta G = -10.3$ kcal mol^{-1}. The associative mechanism predicts the formation of (*R*)-**6a** in 97% ee (at 233.15 K) for an enantiopure catalyst, which is in a good agreement with the experimental value of 87% ee (Table 1, entry 1) attained with the catalyst of 98% ee. Significantly, the dissociative route favors the formation of the opposite, that is, (*S*)-enantiomer.[59] Assuming that both mechanisms operated concurrently, the calculations would predict the formation of (*R*)-**6a** in 53% ee.

In the case of *p*-methoxybenzaldehyde **1h**, the associative mechanism is even more favored with the TS barriers $\Delta G^{\ddagger}_{\text{assoc}} = 26.1$ (*R*) and 26.9 (*S*) kcal mol^{-1}, while the corresponding values for the dissociative pathway are $\Delta G^{\ddagger}_{\text{dissoc}} = 29.3$ (*R*) and 29.7 (*S*) kcal mol^{-1}. Significantly, the energy gap between the (*R*)- and (*S*)-reaction channels in the associative mechanism for **1h** is reduced to 0.8 kcal mol^{-1} and predicts the formation of (*R*)-**6h** in 62% ee (at 273.15 K; in a very good agreement with 45% ee observed experimentally at this temperature; Table 1, entry 18). Note that a higher TS barrier for the formation of (*R*)-**6h** compared to (*R*)-**6a** correlates well with the experimentally observed higher reaction rates of **1a** versus **1h**.

The calculations further show that in the TS the methoxynaphthalene unit of QUINOX (**9**) and the phenyl ring of benzaldehyde (**1a**) are arranged in a parallel orientation, which makes the TS for QUINOX lower in energy than that for the simple pyridine *N*-oxide by 3–5 kcal mol^{-1}.[60] This value is comparable with the strength of the aromatic interaction between benzaldehyde and the catalyst expected in the TS arrangement. Moreover, the difference in the attractive $\pi-\pi$ interactions between the (*R*)- and (*S*)-transition states also constitutes the largest contribution to the enantiodifferentiation since the calculated difference in the dispersion energy stabilizations between the (*R*)- and (*S*)-enantiomers amounts to 1.1 kcal mol^{-1}.[61,62]

Conclusions

The kinetic and computational data indicate that the allylation of aldehydes **1** with allyltrichlorosilanes **2–4**, catalyzed by QUINOX (**9**), is likely to proceed via an associative pathway involving neutral, octahedral silicon complex **22**. In contrast to catalysis by chiral monodentate phosphoramides, such as **10**, only one molecule of QUINOX (**9**) is involved in the rate- and selectivity-determining step. The reaction presumably proceeds via a cyclic chairlike[63] transition state **5** and is characterized by high enantio- and diasteroselectivity. A drop in enantioselectivity observed in the case of electron-rich substrates apparently originates from narrowing the energy gap between the (*R*)- and (*S*)-reaction channels in the associative mechanism (**22**).

Acknowledgment. The paper is dedicated to Professor Victor Sniečkus on the occasion of his 70th birthday. We thank the EPSRC for Grant No. GR/T27051/01, the Ministry of Education and Science of Spain for a fellowship to P. R.-L., the Ministry of Education of the Czech Republic (MŠMT ČR) for Grant No. LC512, the Grant Agency of the Czech Republic for Grant No. 203/08/0350, the European Socrates-Erasmus exchange program for scholarships to L.B. and L.D., Dr. Alfred Bader for an additional support, and Dr. DeLiang Long for the X-ray structure determination. We also thank Profs. Guy C. Lloyd Jones and Pavel Hobza for helpful discussions.

Supporting Information Available: Complete ref 55, general experimental methods, representative allylation and crotylation procedures, NMR spectra of new compounds, all kinetic data and the equilibrium structures, and energies of all the computationally studied species. This material is available free of charge via the Internet at http://pubs.acs.org.

JA711338Q

(58) Lowering the barrier by 4.2 kcal mol^{-1} for the (*R*) reaction channel (compared to the uncatalyzed reaction) corresponds to a $\sim 10^3$ increase of the reaction rate, which is in agreement with the experimental observations.

(59) There is an uncertainty in the translational entropy of the Cl^- ion, which has to be taken into account in the dissociative reaction mechanism; however, this factor is unlikely to affect the overall picture significantly.

(60) The TS barrier calculated for the reaction of benzaldehyde and allyltrichlorosilane catalyzed by pyridine *N*-oxide is $\Delta G^{\ddagger} = 27.5$ kcal mol^{-1}.

(61) Decomposition of the energy differences in the free energy barriers in the associative mechanism between the (*R*) and (*S*) enantiomers (in kcal mol^{-1}) are as follows: in vacuo energies $\Delta E_{\text{gp}} = 0.3$; solvation free energies $\Delta G_{\text{solv}} = -0.7$; in vacuo entropic terms $\Delta(-T\Delta S)_{\text{gp}} = -0.5$; and dispersion energy stabilizations $\Delta E_{\text{disp}} = -1.1$.

(62) Computational analysis of $\pi-\pi$ interactions on the truncated system [benzene−naphthalene] using the TS(*R*) and TS(*S*) geometries (Fig. 4), where benzene and naphthalene represented respective interacting parts of benzaldehyde and QUINOX, produced the interaction energies $\Delta E = -2.8$ (*R*) and −2.6 (*S*) kcal mol^{-1}. In the real system, the difference in arene−arene interactions energies for (*R*)- and (*S*)-manifolds is expected to further increase.

(63) According to the calculations carried out for **1a** and **1h**, the chair conformation is preferred over the twisted boat for both (*R*)-and (*S*)-channels by about 1.5–2.0 kcal mol^{-1}.